Abundant pre-industrial carbon detected in Canadian Arctic headwaters: implications for the permafrost carbon feedback

Environmental Research Letters

LETTER

Abundant pre-industrial carbon detected in Canadian Arctic headwaters: implications for the permafrost carbon feedback

J F Dean[1,2,9], Y van der Velde[2], M H Garnett[3], K J Dinsmore[4], R Baxter[5], J S Lessels[6], P Smith[7], L E Street[8], J-A Subke[1], D Tetzlaff[6], I Washbourne[1], P A Wookey[1] and M F Billett[1]

1 Biological and Environment Sciences, University of Stirling, Stirling FK9 4LA, United Kingdom
2 Department of Earth Sciences, Vrije Universiteit Amsterdam, 1081 HV Amsterdam, Netherlands
3 NERC Radiocarbon Facility, East Kilbride G75 0QF, United Kingdom
4 Centre for Ecology and Hydrology, Penicuik EH26 0QB, United Kingdom
5 Department of Biosciences, University of Durham, Durham DH1 3LE, United Kingdom
6 Northern Rivers Institute, University of Aberdeen, Aberdeen AB24 3UF, United Kingdom
7 Institute of Biological and Environmental Sciences, University of Aberdeen, Aberdeen AB24 3UU, United Kingdom
8 School of Geosciences, University of Edinburgh, Edinburgh, EH9 3FF, United Kingdom
9 Author to whom any correspondence should be addressed.

E-mail: j.f.dean@vu.nl

Keywords: carbon dioxide CO_2, dissolved organic carbon DOC, methane CH_4, Arctic catchments, inland waters, radiocarbon ^{14}C

Supplementary material for this article is available online

OPEN ACCESS

RECEIVED
8 September 2017

REVISED
9 December 2017

ACCEPTED FOR PUBLICATION
15 December 2017

PUBLISHED
27 February 2018

Abstract

Mobilization of soil/sediment organic carbon into inland waters constitutes a substantial, but poorly-constrained, component of the global carbon cycle. Radiocarbon (^{14}C) analysis has proven a valuable tool in tracing the sources and fate of mobilized carbon, but aquatic ^{14}C studies in permafrost regions rarely detect 'old' carbon (assimilated from the atmosphere into plants and soil prior to AD1950). The emission of greenhouse gases derived from old carbon by aquatic systems may indicate that carbon sequestered prior to AD1950 is being destabilized, thus contributing to the 'permafrost carbon feedback' (PCF). Here, we measure directly the ^{14}C content of aquatic CO_2, alongside dissolved organic carbon, in headwater systems of the western Canadian Arctic—the first such concurrent measurements in the Arctic. Age distribution analysis indicates that the age of mobilized aquatic carbon increased significantly during the 2014 snow-free season as the active layer deepened. This increase in age was more pronounced in DOC, rising from 101–228 years before sampling date (a 120%–125% increase) compared to CO_2, which rose from 92–151 years before sampling date (a 59%–63% increase). 'Pre-industrial' aged carbon (assimilated prior to ~AD1750) comprised 15%–40% of the total aquatic carbon fluxes, demonstrating the prevalence of old carbon to Arctic headwaters. Although the presence of this old carbon is not necessarily indicative of a net positive PCF, we provide an approach and baseline data which can be used for future assessment of the PCF.

1. Introduction

It is estimated that Arctic permafrost soils contain between 1330 and 1580 Pg organic carbon (C) (Schuur *et al* 2015), equivalent to roughly half the total fossil fuel C emissions since the start of the Industrial Revolution (~AD1750, Boden *et al* 2010). Rising air temperatures in the Arctic are warming permafrost soils, which can lead to deepening of the seasonally thawed 'active' layer (AL), and exposure of previously frozen organic matter to *in-situ* mineralization and lateral transport (Schuur *et al* 2009, Vonk *et al* 2013a 2013b, Abbott *et al* 2016). The organic C stored in permafrost can be up to, or greater than, ~50 000 years old, having been fixed into plant matter during past snow-free seasons and accumulating in soils (Mann *et al* 2015).

Arctic headwater streams, ponds and lakes are closely connected to the landscape via hydrological flow paths, both along the surface and through the AL

(Paytan *et al* 2015, Dean *et al* 2016), and consequently carry signals of change in permafrost conditions (Neff *et al* 2006, Raymond *et al* 2007). Old C (defined here as C assimilated into plant material from the atmosphere and sequestered in organic-rich soils prior to the 1950s) has proven notoriously difficult to detect in aquatic systems due to the overwhelming presence of 'modern' C (assimilated since 1950). Post-1950s C has a significantly enriched ^{14}C signature as a result of atmospheric nuclear weapons testing (Dutta 2016). This ^{14}C enrichment has severely hindered attempts to provide high resolution dating of C assimilated over the past ~200 years, especially when the material is derived from multiple years (Evans *et al* 2014). Only systems affected by significant permafrost thaw, usually in the form of rapid thaw-related erosion (thermokarst), have shown clear signals of old dissolved or particulate organic C (DOC and POC, respectively) being mobilized (Vonk *et al* 2015).

Recent studies highlight headwater systems as hotspots for preferential mineralization of old DOC during transport (Drake *et al* 2015, Spencer *et al* 2015), resulting in the release of greenhouse gases (GHGs) driving the 'permafrost carbon feedback' (PCF, Walter Anthony *et al* 2016). However, the release of GHGs derived from old permafrost C has only been inferred by aquatic ^{14}C studies of DOC and POC, with the few studies that consider aquatic GHG ^{14}C signatures themselves focusing only on ebullition fluxes, and none combining these measurements (Negandhi *et al* 2013, Bouchard *et al* 2015, Walter Anthony *et al* 2016).

To address this, we measured the ^{14}C content of CO_2 alongside DOC in a range of inland headwaters (streams, ponds and lakes) in the western Canadian Arctic to determine the contribution of old permafrost C to these C fluxes. Additional sampling of $^{14}CH_4$ at two locations supplemented the assessment of C sources in GHG fluxes from headwaters draining permafrost soils. $^{14}CO_2$ and $^{14}CH_4$ samples were collected using newly developed techniques, and alongside $DO^{14}C$, represent the first such combined aquatic ^{14}C measurements in the Arctic. Previous work at the study site showed that the main pathway of water delivery to the streams and lakes is via the organic-rich soils, which can be up to 50 cm deep and contain maximum bulk organic C ages of 2200–6200 years B.P. (Quinton and Pomeroy 2006, Dean *et al* 2016). Here, we focus on the aquatic mobilization of C assimilated prior to the Industrial Revolution, as it is demonstrably older than the AD1950 'old C' cut-off.

2. Methods

2.1. Sample collection and analysis

Samples were collected from a series of headwater systems (six lake sites, four stream sites and four pond sites) from a ~14 km^2 area in the continuous permafrost zone of the Northwest Territories, Canada (68° 44′ 54.5″ N, 133° 29′ 41.7″ W; figure 1). The main study catchment within this area is Siksik Creek (0.94 km^2), which forms part of the Trail Valley Creek catchment. The study site is an upland tundra, consisting of hummock and inter-hummock morphology, where the inter-hummocks are loosely filled by organic matter and act as the dominant hydrologic pathway in the system; the hummocks are primarily formed from mineral soils (Quinton and Pomeroy 2006, Dean *et al* 2016). The aquatic biogeochemistry of the site is dominated by the organic inter-hummocks (Quinton and Pomeroy 2006, Dean *et al* 2016).

The catchments are predominately covered in dwarf and low shrubs, sedges (*Eriophorum* and *Carex* spp.), bryophytes and lichens, with some tall shrub patches (*Alnus viridis* and *Betula* spp.) on the hillslopes. The riparian zones are vegetated with *Betula glandulosa* and *Salix* spp. The region belongs to the Circumpolar Arctic Vegetation Map (Walker *et al* 2005) bioclimate sub-zone E, and is dominated by low-shrub tundra (map unit S2) out-with riparian zones. While the study site is considered to be relatively pristine (Dean *et al* 2016), the annual average air temperature in Inuvik (c. 45 km south of the study site) has increased by 2.5 °C since 1970, and active layer depths at Illisarvik on Richards Island, c. 120 km north-northwest of the site, have increased by around 8 cm since 1983 (Burn and Kokelj 2009).

Aquatic sampling took place in the snow free season of 2014. Repeated sampling took place within Siksik creek catchment, with the main stream and two polygon sites sampled five times throughout the season (figure 1). A series of lake and polygon sites outside Siksik catchment were sampled once in August 2014 (figure 1). Samples for DOC, CO_2 and CH_4 concentrations and isotopic content were collected at each site (see supplementary methods; Dean *et al* 2016). 500 ml water samples were collected and filtered for $DO^{14}C$ analysis ($n = 26$). $^{14}CO_2$ ($n = 36$) and $^{14}CH_4$ ($n = 2$) samples were collected by equilibrating sample waters with a large headspace, following Garnett *et al* (2016a), (2016b)—see supplementary methods. Low CH_4 concentrations prevented $^{14}CH_4$ sample collection on all but two occasions (figure 2(*c*); Dean *et al* 2017).

2.2. Age distribution analysis

Aquatic ^{14}C samples represent an integrated signal from the upstream catchment area, and therefore a source-apportionment approach (such as an age distribution) should be used to describe the relative contributions of C from different soil layers and locations within the catchment (Sierra *et al* 2017). We therefore applied the approach described below to represent soil C export dynamics at the catchment scale.

At the end of each growing season, the organic matter from senescing vegetation contributes to the upper soil layers, although deep rooting of vegetation will contribute C to a range of depths, both through exudations and root turnover (meaning that age

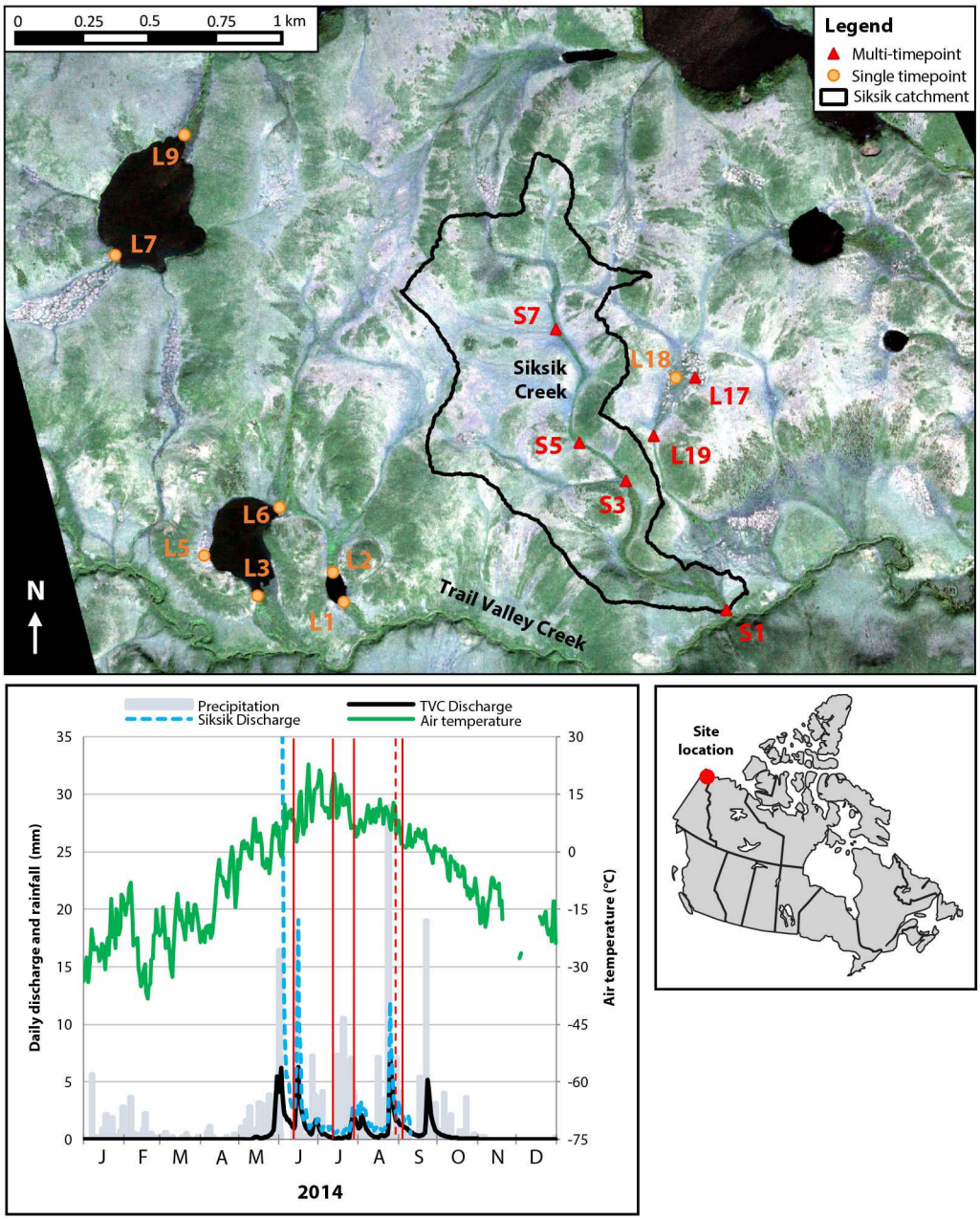

Figure 1. Top—site locations for the single and multi-timepoint ^{14}C sampling points; 'S' indicates stream sites, 'L' indicates lake or polygon sites (see table 1). Bottom right—the location of the study area in NWT, Canada. Bottom left—the hydroclimatic conditions during the 2014 sampling campaigns; the solid vertical red lines represent multi-timepoint sampling, and the dashed red line represents the wider lake survey timepoint; data from Environment Canada (Trail Valley Creek; TVC), and the gauging station built in this study (see supplementary methods).

estimates derived with an exponential distribution are conservative, as dilution with recent C is deeper than assumed by this approach). This occurs each year, and results in the formation of organic soil horizons across the Arctic tundra. Each year's input of plant-derived organic matter loses C through the activities of detritivores and decomposers, as well as through leaching, exporting progressively less C per year over time as the residual organic matter tends to become more recalcitrant. Here, based upon previous work (Raymond *et al* 2007, Moore *et al* 2013, Evans *et al* 2014), we chose an exponential distribution to represent these soil dynamics (equation (1)), assuming that the largest C contributions come from the upper youngest soil layers, and that the contribution from each successive older soil layer decreases exponentially as they become thinner through time (Raymond *et al* 2007, Moore *et al* 2013, Evans *et al* 2014)—note that changes in lability of C at increasing depth can also be anticipated, but defining a simple relationship may be elusive, based on current understanding (Jansson and Taş 2014, Ward and Cory 2015) (calculations made in R, version 3.3.2; figures 2(*a*) and (*b*)).

A more sophisticated distribution is not necessarily better due to the complex and highly heterogeneous soil age profiles that exist within even small stream

Table 1. ^{14}C values for each sampling point (percent modern C [pmC] and conventional ^{14}C age in years B.P.), and associated numerical age distribution outputs ('solution'—years before sampling date [years BSD]); uncertainties in the pmC values reflect the uncertainty from the AMS instrument and sample preparation; uncertainties in the age distribution output reflect the propagation of this error into the age distribution analysis.

			$^{14}CO_2$				DO^{14}C			
					Age distribution (years BSD)				Age distribution (years BSD)	
Site	Water type	Sampling date (2014)	^{14}C (pmC $\pm 1\sigma$)	Conv. Age (y B.P.)	Younger solution	Older solution	^{14}C (pmC $\pm 1\sigma$)	Conv. Age (y B.P.)	Younger solution	Older solution
S1	Stream	12/06	105.06 ± 0.51	modern	no sol.	120 ± 63	105.53 ± 0.49	modern	3 ± 58	113 ± 51
S3	Stream	12/06	108.52 ± 0.49	modern	7 ± 1	76 ± 5	106.45 ± 0.53	modern	4 ± 1	100 ± 7
S5	Stream	12/06	—	—	—	—	106.87 ± 0.50	modern	5 ± 1	94 ± 6
S7	Stream	12/06	108.97 ± 0.49	modern	7 ± 1	71 ± 5	109.64 ± 0.48	modern	8 ± 1	65 ± 4
L17	Polygon	12/06	106.72 ± 0.47	modern	5 ± 1	96 ± 6	104.45 ± 0.49	modern	no sol.	131 ± 9
L19	Polygon	12/06	106.66 ± 0.48	modern	5 ± 1	97 ± 6	106.16 ± 0.49	modern	4 ± 1	104 ± 7
S1	Stream	13/07	103.88 ± 0.48	modern	no sol.	142 ± 9	—	—	—	—
S3	Stream	13/07	104.57 ± 0.48	modern	no sol.	129 ± 9	—	—	—	—
S5	Stream	12/07	104.70 ± 0.48	modern	no sol.	126 ± 9	—	—	—	—
S7	Stream	12/07	105.45 ± 0.49	modern	3 ± 59	114 ± 51	—	—	—	—
L17	Polygon	12/07	104.40 ± 0.46	modern	no sol.	132 ± 9	—	—	—	—
L19	Polygon	12/07	104.16 ± 0.48	modern	no sol.	137 ± 8	—	—	—	—
S1	Stream	28/07	103.95 ± 0.46	modern	no sol.	140 ± 9	—	—	—	—
S3	Stream	28/07	103.84 ± 0.48	modern	no sol.	142 ± 9	—	—	—	—
S5	Stream	28/07	103.10 ± 0.45	modern	no sol.	158 ± 10	—	—	—	—
S7	Stream	28/07	104.56 ± 0.48	modern	no sol.	129 ± 9	—	—	—	—
L17	Polygon	25/07	104.90 ± 0.48	modern	no sol.	123 ± 64	—	—	—	—
L19	Polygon	26/07	104.02 ± 0.46	modern	no sol.	138 ± 9	—	—	—	—
S1	Stream	30/08	103.62 ± 0.48	modern	no sol.	147 ± 9	100.64 ± 0.88	modern	no sol.	219 ± 25
S3	Stream	30/08	104.20 ± 0.45	modern	no sol.	136 ± 8	100.66 ± 0.88	modern	no sol.	218 ± 25
S5	Stream	30/08	104.86 ± 0.49	modern	no sol.	123 ± 65	101.07 ± 0.88	modern	no sol.	210 ± 24
S7	Stream	30/08	104.89 ± 0.49	modern	no sol.	123 ± 64	101.57 ± 0.89	modern	no sol.	195 ± 23
L17	Polygon	29/08	102.17 ± 0.47	modern	no sol.	179 ± 12	97.37 ± 0.85	214 ± 70	no sol.	336 ± 37
L18	Polygon	29/08	103.01 ± 0.45	modern	no sol.	160 ± 10	100.73 ±0.88	modern	no sol.	216 ± 25
L19	Polygon	29/08	104.23 ± 0.48	modern	no sol.	135 ± 9	100.76 ± 0.88	modern	no sol.	219 ± 25
L1	Lake	01/09	104.43 ± 0.48	modern	no sol.	131 ± 9	101.59 ± 0.89	modern	no sol.	194 ± 23
L2	Lake	01/09	104.78 ± 0.49	modern	no sol.	125 ± 65	100.27 ± 0.87	modern	no sol.	230 ± 26
L3	Lake	01/09	100.94 ± 0.47	modern	no sol.	214 ± 12	101.05 ± 0.88	modern	no sol.	210 ± 24
L5	Polygon	01/09	105.44 ± 0.49	modern	3 ± 59	114 ± 51	99.72 ± 0.87	22 ± 70	no sol.	248 ± 28
L6	Lake	01/09	105.15 ± 0.49	modern	no sol.	119 ± 62	100.76 ± 0.88	modern	no sol.	219 ± 25
L7	Lake	02/09	104.09 ± 0.48	modern	no sol.	138 ± 9	100.94 ± 0.88	modern	no sol.	214 ± 24
L9	Lake	02/09	98.03 ± 0.45	160 ± 37	no sol.	311 ± 18	98.98 ± 0.86	82 ± 70	no sol.	277 ± 32
S1	Stream	08/09	—	—	—	—	102.16 ± 0.89	modern	no sol.	179 ± 23
S3	Stream	08/09	103.48 ± 0.45	modern	no sol.	149 ± 9	100.67 ± 0.88	modern	no sol.	218 ± 25
S5	Stream	08/09	104.25 ± 0.45	modern	no sol.	135 ± 9	102.11 ± 0.89	modern	no sol.	181 ± 23
S7	Stream	08/09	105.53 ± 0.46	modern	3 ± 58	113 ± 51	103.06 ± 0.90	modern	no sol.	158 ± 20
L17	Polygon	08/09	102.96 ± 0.48	modern	no sol.	161 ± 11	97.15 ± 0.85	233 ± 70	no sol.	345 ± 35
L19	Polygon	08/09	103.35 ± 0.48	modern	no sol.	152 ± 10	98.98 ± 0.86	83 ± 70	no sol.	277 ± 32

			$^{14}CH_4$			
					Age distribution (years BSD)	
Site	Water type	Sampling date (2014)	^{14}C (pmC $\pm 1\sigma$)	Conv. Age (y B.P.)	Young solution	Old solution
S3	Stream	13/07	100.78 ± 1.00	modern	no sol.	218 ± 57
L17	Polygon	25/07	72.23 ± 0.89	2613 ± 102	no sol.	2168 ± 199

modern = no conventional radiocarbon age possible when >100 pmC; no sol. = no younger solution available from the age distribution analysis.

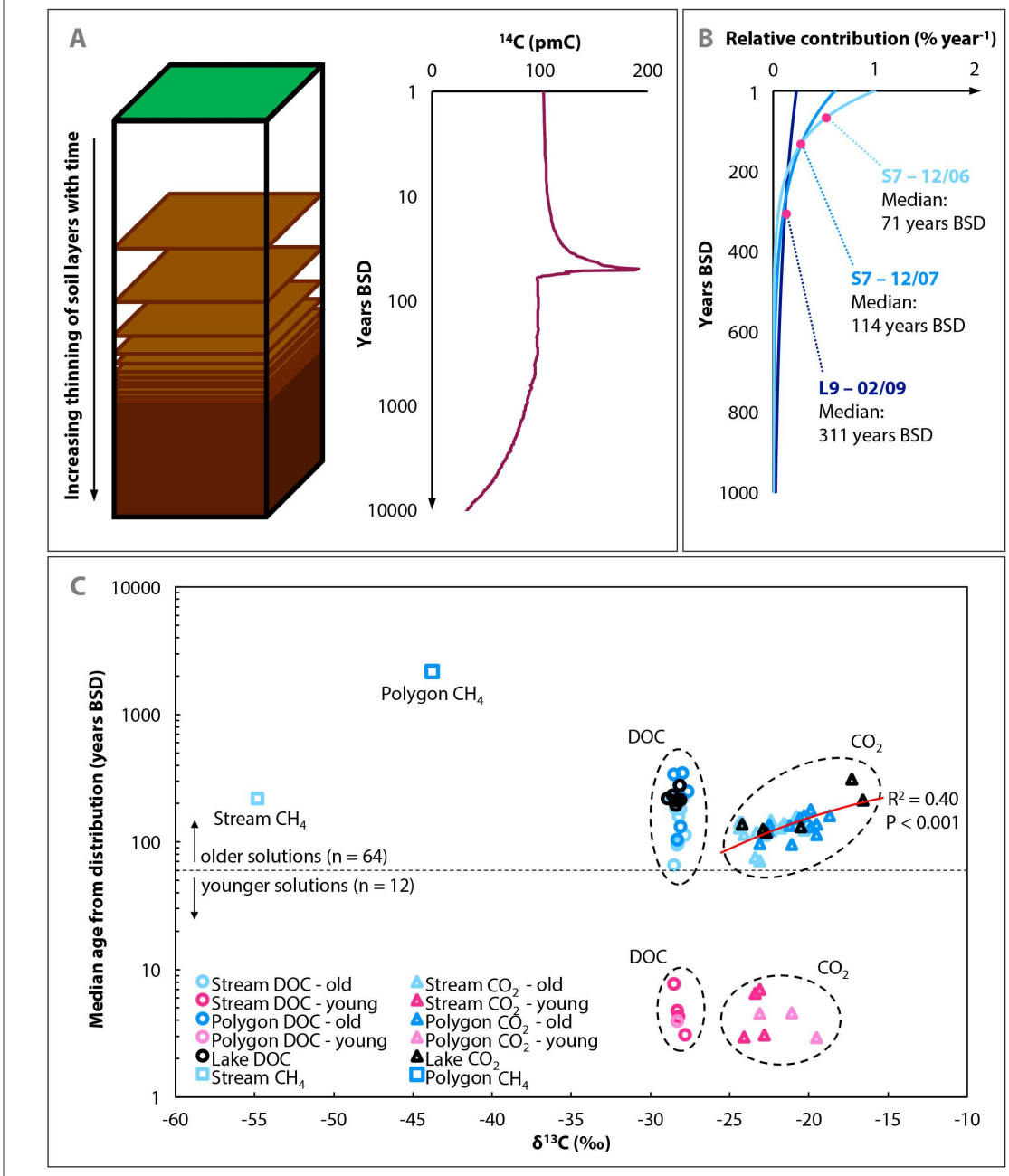

Figure 2. Schematic of the exponential distribution of C in a given water sample, and the age and $\delta^{13}C$ of DOC, CO_2 and CH_4 samples collected in this study. (*a*) The contribution of C from different layers is assumed to decrease exponentially with depth as C is degraded and lost from the soil profile over time. Each soil layer has a specific ^{14}C signature based on the atmospheric $^{14}CO_2$ at the time when C was fixed, and the radioactive decay that has occurred since fixation. This results in different proportions of C ages contributing to a given water sample. (*b*) Bulk ^{14}C signatures of DO^{14}C, $^{14}CO_2$ and $^{14}CH_4$ (table 1), are assigned a median age (pink dots) based on the exponential distribution that matches the measured bulk ^{14}C signature (three examples are shown for $^{14}CO_2$; see table 1). (*c*) Measured median ^{14}C ages in years before sampling date (years BSD), based on the assumed age distributions in the catchments soils. For some samples ($n = 12$), the age distributions have both a younger and an older numerical solution due to the influence of atmospheric nuclear bomb testing during the 1950s and 1960s on global atmospheric $^{14}CO_2$ values (indicated by dashed horizontal line). A linear trend line (which appears curved due to the logarithmic *y*-axis) is shown for the old CO_2 solutions, indicating a positive relationship between $\delta^{13}C$ and age in the CO_2 samples.

catchments, and therefore detailed soil profile data can be challenging to extrapolate at the catchment scale in a way that is relevant to hydrological export (Hrachowitz and Clark 2017). We assume that the youngest C contribution is from the 2013 soil layers, as the majority of soil organic matter accumulation occurs at the end of the growing season during plant senescence (Raymond *et al* 2007), but incorporating potential contributions from the sampling year (2014 in this study) into these distributions had a negligible impact on the derived median ages. We assigned each soil layer a ^{14}C value in pmC based on atmospheric $^{14}CO_2$ values during past northern hemisphere summers (NH zone 1) (Hua *et al* 2013, Levin *et al* 2013, Reimer *et al* 2013), representing the ^{14}C signature of the CO_2 fixed into vegetation during the growing season.

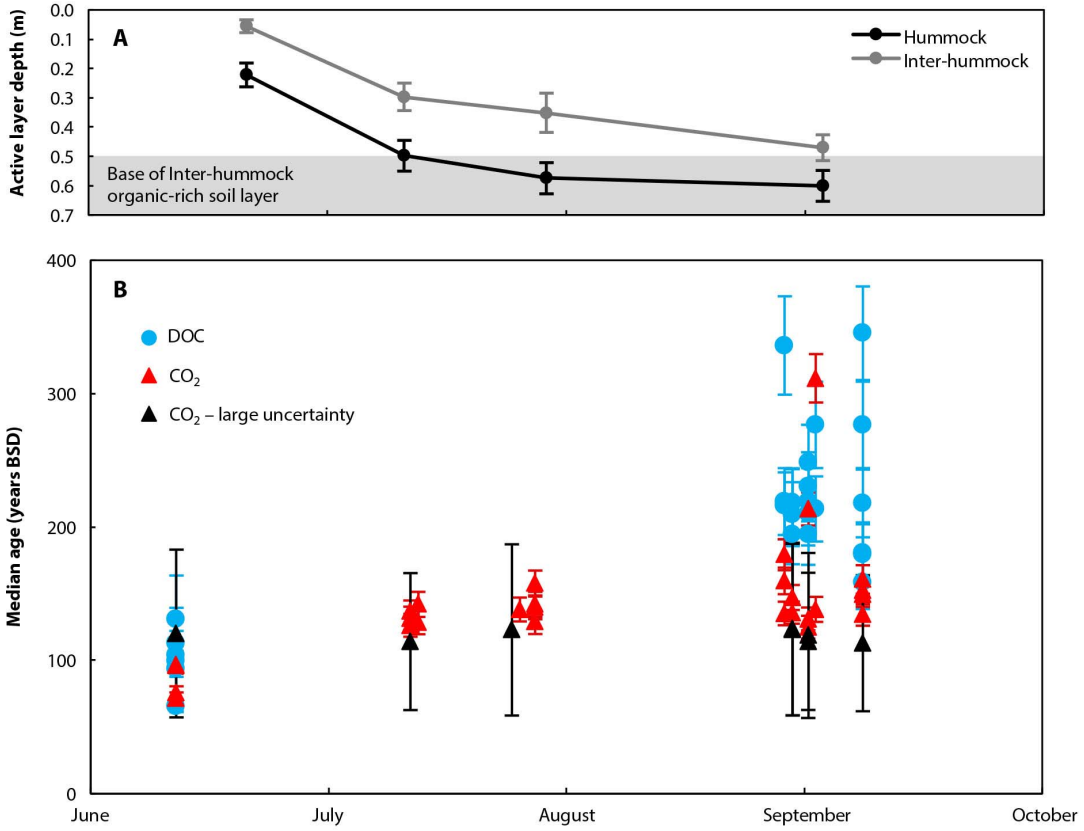

Figure 3. (*a*) Active layer depth in Siksik catchment during the 2014 growing season (Dean *et al* 2016); the depth of the organic soil layer base in the inter-hummocks is indicated by the grey shaded area. (*b*) The ^{14}C timeline of DOC and CO_2 during the growing season, showing only age distribution solutions with older median ages (see figure 2(*c*) and section 3). Uncertainty ranges indicate the propagation of the analytical uncertainty into the age distribution analysis (table 1), which in some cases resulted in large uncertainties (plotted separately in black triangles) inherent in the age distributions (see section 3).

Published records only go up to 2012; values for 2013–14 were generated assuming the same rate of depletion in atmospheric $^{14}CO_2$ as occurred between 2011 and 2012. This approach assumes unlimited organic matter depth in the soil profile; we did not assign a maximum basal age as in Moore *et al* (2013) and Evans *et al* (2014), but no sample's age distribution in this study incorporated any C older than the known maximum age at the site (2200–6200 years B.P), with the exception of the oldest CH_4 sample (table 1).

To determine the exponential distribution for the measured ^{14}C content of each sample, we solved equation 1 for λ (the rate parameter):

$$\mathrm{pmC}_{\mathrm{stream}}(t) = \int_0^{\inf} \lambda e^{-\lambda T}\, \mathrm{pmC}_{\mathrm{air}}(t-T)\, 2^{\frac{T}{5730}}\, \mathrm{d}T \quad (1)$$

where $\mathrm{pmC}_{\mathrm{stream}}$ is the aquatic sample's measured ^{14}C content in percent modern carbon (pmC), $\mathrm{pmC}_{\mathrm{air}}$ is the atmospheric $^{14}CO_2$ content in pmC at time (t), and T is the age of the sample in 'years before sampling date' (years BSD; i.e. years before 2014 in this study), and should not be confused with conventional radiocarbon ages reported in years B.P. All aquatic ages in the manuscript are given in years BSD based on the distributions, with years B.P. values confined to the conventional ^{14}C reporting in table 1 and the supplementary information available at stacks.iop.org/ERL/13/034024/mmedia. Note that λ can have two solutions in some circumstances (see section 3).

Each sample of DOC, CO_2 and CH_4 had a bulk ^{14}C value in pmC which can be described by a single exponential distribution of soil ^{14}C contributions (figure 2(*b*)). We report the median value of the distribution (years BSD, figure 2(*b*)), which has an intuitive interpretation: Half of the C is younger and half of the C is older than this median age. The mean of an exponential distribution gives an older age than the median by a factor of 1.44 (equation (2)).

$$\text{Median Age} = \lambda^{-1} \ln(2). \quad (2)$$

We incorporate the analytical uncertainty of each individual sample's ^{14}C value (table 1) into a median uncertainty range (figure 3, table 1). In some cases, both a young and an old distribution can describe a given sample's ^{14}C content. In figure 3 and in the statistical analyses we use only the old distributions due to the prevalence of old C in the system throughout the study period (see section 3).

3. Young versus old solutions to the ^{14}C age distributions

In June, following the spring snow melt, nine out of the 11 samples have ^{14}C values (in pmC) that are only slightly above the atmospheric $^{14}CO_2$ signature at the time of sampling (103.12 pmC for this study). This means that the ^{14}C values of these samples can represent C assimilated either side of the atmospheric ^{14}C bomb peak (figure 2(*b*)). Therefore, two possible exponential distributions can describe their ^{14}C value, giving both a younger (i.e. 3–8 years old) and an older (i.e. > 70 years old) solution. The aquatic C in the study system in June could therefore be very young, sourced primarily from net primary production in the last few years (Raymond *et al* 2007) or from C fixed predominantly just prior to the bomb-peak (Evans *et al* 2014). In some cases (DOC, $n = 1$; CO_2, $n = 8$), the analytical uncertainty propagated into the age distributions results in a high uncertainty as the distribution cannot distinguish between the old and young solutions (figure 3).

For the June samples, we cannot definitively conclude that one solution is correct over the other. Raymond *et al* (2007) concluded that the younger solution is most likely following the spring melt, as the AL is shallow, and snow melt will flush out a pulse of modern C from recently accumulated material and microbial biomass in the upper unfrozen soil layers. However, two samples at this time point (one DOC and one CO_2, but from different sites) cannot have a younger solution, indicating that there is significant C in these samples derived from pre-bomb peak material—this may be due to flushing of old C mobilized at the end of the previous season during the snow melt. After this time point, no younger distributions can describe the $DO^{14}C$ samples, and only three $^{14}CO_2$ samples can have younger distributions (table 1). Evans *et al* (2014) suggest that the younger solution in these scenarios is more likely given the undisturbed history of the site (Dean *et al* 2016). But based on our results showing that younger solutions are not possible for the substantial majority of samples after June, we assume the older solutions are also more likely for the early season samples given that this assumption yields a smooth increase in age over the season, as opposed to a jump in age between early and late season. A jump in age from predominantly young C being exported in June to older C later in the season is not reflected in the seasonal evolution of the DOC, CO_2 or CH_4 concentrations (supplementary figure S2), or the overall aquatic biogeochemistry (Dean *et al* 2016). Further, the positive relationship between $\delta^{13}C$ and CO_2 age ($R^2 = 0.40$, $P < 0.001$; figure 2(*c*)) also indicates that some of the CO_2 in the water samples is produced at depth (this increase in $\delta^{13}C$ with depth is due either to the mineralization of C deeper in the soil profile that generally has a higher $\delta^{13}C$ value, or isotopic fractionation by methanogenesis in the deeper, less oxic soil layers; Clymo and Bryant 2008, Corbett *et al* 2013, Hicks Pries *et al* 2013), supporting the exclusion of the younger distributions as deeper peat layers will generally contain older C. However, even if the younger solutions are assumed to be correct in the June samples, this would only further emphasize the seasonal evolution of C age exported by the study waters seen in figure 3. Further, it should be noted that the old solutions still contain a substantial proportion of young C (figure 2(*b*)).

Thus, earlier in the season, young C may form a significant component of the aquatic DOC and CO_2 export, but the seasonal evolution of the $DO^{14}C$ and $^{14}CO_2$ in the system demonstrates that old C becomes more prevalent later in the season (figures 3 and 4). In the following analysis, we assume that the older solutions are true.

4. Increasing age of aquatic carbon over the growing season

The ^{14}C age distributions indicate the prevalence of old C in most samples collected in this study (figure 2(*c*), table 1). DOC and CO_2 ages were youngest in June following the spring snow-melt, and were not significantly different ($P = 0.27$, figure 3). By August/September, on average, CO_2 ages had risen from 92–151 years BSD (59%–63% increase, confidence interval: 37%–94%, see supplementary methods), while DOC ages rose from 101–228 years BSD (120%–125% increase, confidence interval: 70%–185%), showing an increase over the season that is more pronounced in the DOC than CO_2 (figure 3).

However, the seasonal increase in C age was not matched by an equivalent trend in aquatic DOC, CO_2 or CH_4 concentrations at the sites sampled for ^{14}C analyses in 2014 (supplementary figure S2), or across the entire study area in 2013–2014 (Dean *et al* 2016). The observed age increase represents proportionately higher contributions from older soil layers later in the season that would be undetectable without ^{14}C.

The majority of C in both CO_2 and DOC in our samples (60%–85%) was fixed in the industrial era post ~AD1750 (figure 4). However, the modeled relative contribution of C fixed in the pre-industrial era increased from 15% to a maximum of 40% over the growing season, demonstrating the mobilization of old C in both DOC and CO_2 as the thaw front deepened. Seasonal increases in contributions of C from older soil layers to respired CO_2 have also been observed in the Alaskan tundra (Hicks Pries *et al* 2013), demonstrating parallels between terrestrial and aquatic CO_2 export in permafrost zones. This contrasts with recent work in an organic-rich permafrost-free boreal catchment in northern Sweden, where little seasonal variability was seen in the age of aquatic DOC, CO_2 and CH_4 export, showing that aquatic C export from non-permafrost catchments can differ significantly (Campeau *et al* 2017a).

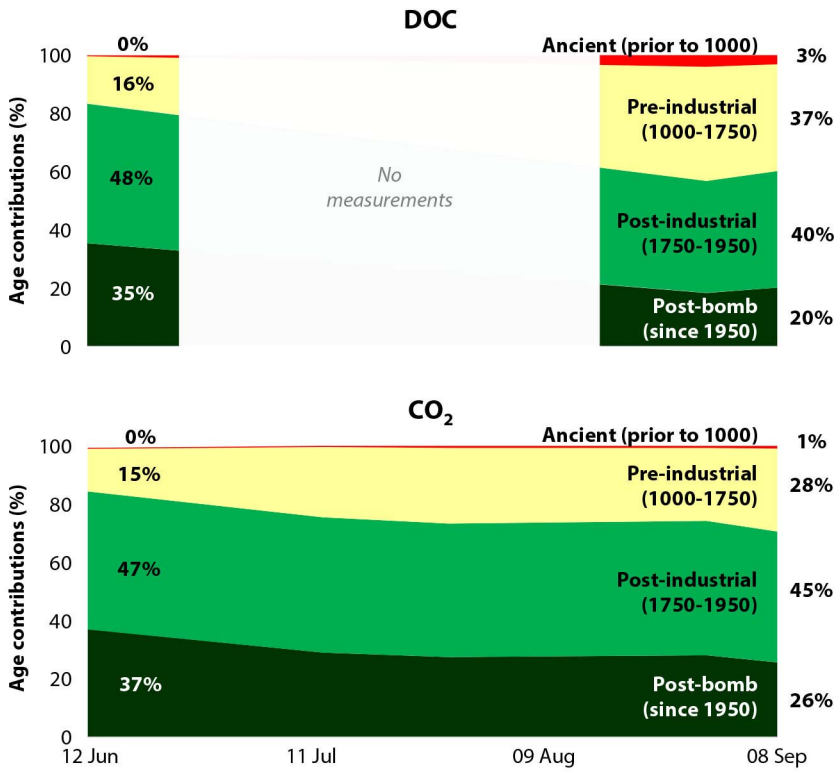

Figure 4. Relative proportions of C of different ages (years AD) to aquatic DOC (top) and CO_2 (bottom) through the 2014 growing season, assuming the older solutions from the age distributions early in the season are true (section 3).

There is a significant positive correlation between DOC and CO_2 age ($P < 0.01$; $R^2 = 0.38$), but DOC is generally older than CO_2, and there is a clear difference in $\delta^{13}C$ between CO_2 and DOC samples (figure 2(*c*)). It is possible that CO_2 is younger than DOC due to the intrusion of atmospheric CO_2 into the study waters, and that ^{13}C fractionation may occur during this process (Doctor *et al* 2008). However, aquatic CO_2 concentrations were consistently much higher (by a factor of ~11) than atmospheric values (Dean *et al* 2016), suggesting that CO_2 predominantly moves from the water to the atmosphere, rather than the reverse (and by convention, isotopic fractionation of ^{14}C due to invasion is corrected for). The increasing trend between CO_2 age and $\delta^{13}C$ (figure 2(*c*)) indicates a positive relationship between organic C age and its production at depth (see section 3, Clymo and Bryant 2008, Corbett *et al* 2013, Street *et al* 2016). Previous work at the study site indicated that there was limited input to the aquatic biogeochemistry of the site from weathering of the local bedrock and tills (Dean *et al* 2016), and there is no evidence of a carbonate contribution to the $^{14}CO_2$ samples collected in this study (supplementary figure S1), supporting the conclusion that this relationship between ^{14}C and $\delta^{13}C$ in the CO_2 samples is caused by the production of CO_2 at depth in the soil profile.

DOC likely represents C sourced from the entire thawed soil profile due to the vertical infiltration of water that then moves laterally through the soils until discharged into open water. CO_2, however, is predominantly produced by soil organic matter metabolism in the younger, unsaturated soil layers (Hicks Pries *et al* 2016, Street *et al* 2016), with some contribution of CO_2 generated in the older saturated soil layers; increased CO_2 generation from the older deeper layers results in higher $\delta^{13}C$ values compared to $\delta^{13}C$-DOC (Clymo and Bryant 2008, Corbett *et al* 2013, Hicks Pries *et al* 2013). The indication of organic matter degradation at depth in this study is further evidence for the presence of old C in bulk DOC and CO_2 samples, with relative contributions of C from deeper soil layers increasing through the season as the AL deepens (figures 3 and 4).

Only two $^{14}CH_4$ samples could be collected during the sampling campaign due to highly heterogeneous and often low dissolved CH_4 concentrations in this upland tundra study system (supplementary figure S2; Dean *et al* 2016, Street *et al* 2016). A sample collected from a deep ice-wedge polygon (which exposed the oldest soil layers) was much older (2168 ± 199 years BSD) than a stream sample (218 ± 57 years BSD), but both contained a large pre-industrial C component (43%–92%, table 1). This indicates that old C may be exported from the system as CH_4, although both the age and flux may be highly variable.

5. Implications for current understanding of the permafrost carbon feedback

The aquatic ^{14}C ages presented here clearly demonstrate that, as the thaw front advances deeper into the soil profile during the thaw season, older C is mobilized into inland waters as both DOC and CO_2. We also demonstrate the potential for aquatic mobilization of old dissolved CH_4. The export of aged C as aquatic CO_2 is an important finding as direct release of CO_2 can form part of the PCF, whereas the potential for aged DOC to contribute to the PCF depends on its fate during freshwater transport and residence in the ocean (Vonk *et al* 2015).

This first look at dissolved CO_2 age dynamics in Arctic headwaters presented here shows that it generally resembles DOC export (see section 4). However, the disconnect between DOC and CO_2 age and $\delta^{13}C$ suggests that little of the aquatic CO_2 was generated from DOC mineralization in the aquatic zone. The CO_2 is, therefore, most likely generated in the soil profile and transported laterally, in aqueous phase, into the headwater systems (Campeau *et al* 2017b). This contrasts with previous studies that demonstrated the rapid mineralization of old DOC (Vonk *et al* 2013a, Drake *et al* 2015, Mann *et al* 2015, Spencer *et al* 2015); however, these studies were from Arctic regions with extremely old ice-rich yedoma deposits containing C that can be ~50 000 years B.P. or older, whereas the oldest C observed in the present study area was 2200–6200 years B.P. Therefore, inland water ^{14}C age distributions may be significantly different in yedoma regions.

POC, in comparison, is generally older than DOC in aquatic systems (Guo *et al* 2007, Marwick *et al* 2015), and can form a substantial component of the carbon exported by Arctic catchments affected by permafrost thaw, particularly where thermokarst activity is occurring (Vonk *et al* 2015). Thermokarst activity was not observed at our study site, so may not be a major component of C export in the study catchments. However, to fully account for the age of C exported from Arctic aquatic systems, it is important to consider $PO^{14}C$ as well as more extensive $^{14}CH_4$ measurements in future studies.

For pan-Arctic regions where modern aquatic ^{14}C ages are common, the results presented here suggest that up to 30% of CO_2 and 40% of DOC aquatic fluxes (figure 4), equivalent to 16 (range: 6–25) and 10 (range: 5–14) Tg C yr^{-1}, respectively (McGuire *et al* 2009, Holmes *et al* 2012, Vonk *et al* 2015, Wik *et al* 2016), may be derived from organic matter formed in the pre-industrial era. These values can be considered conservative estimates, as the proportion of pre-industrial C observed in this study does not represent POC or CH_4 export, or areas that are affected by more severe permafrost thaw and thermokarst (Olefeldt *et al* 2016), where a larger proportion of old C would be expected in aquatic C fluxes due to the exposure of deep organic matter, especially in yedoma regions (Vonk *et al* 2015, Walter Anthony *et al* 2016).

To check that the aquatic C ages exported from the site, based on the age distributions, are within the right order of magnitude, we apply a basic estimate for the expected C export if the study site were in equilibrium (i.e. the C inputs to the soils as NPP equal soil outputs, and total soil C stocks remain at steady-state; see supplementary methods). Under these assumptions, we would expect to observe median aquatic C ages ranging from 21–117 years BSD, with ~21% of this C of pre-industrial origin. This indicates that the ages we see in the aquatic export from this site are within the expected range. In order to take this analysis a step further and to quantify whether the aquatic C export is contributing to the PCF (i.e. whether the observed ages are significantly older than the expected ages, and therefore inconsistent with a terrestrial C cycle at steady-state), we need a more detailed model of soil age distributions, and to be able to partition the ages of CO_2 and CH_4 lost vertically from the soil versus the lateral aquatic DOC and POC components. The analyses presented here serve as a first step in this direction, and future work should consider upscaling point-source soil data to the catchment scale to relate the measured vertical soil distributions directly to aquatic C export.

There is, therefore, no clear evidence that the aquatic systems in the immediate study area are currently contributing to the PCF. Given this 'baseline' state of the study catchment, the findings presented here suggest that pre-industrial C is already present in substantial amounts in the Arctic C cycle, and that old C export will likely be enhanced by permafrost thaw in response to climate warming.

Acknowledgments

This work was primarily supported by the UK Natural Environment Research Council (NERC), grant numbers NE/K000217/1, NE/K000225/1, NE/K000268/1 and NE/K000284/1. JFD acknowledges partial support by the program of the Netherlands Earth System Science Centre (NESSC), financially supported by the Ministry of Education, Culture and Science (OCW). We would like to thank the Aurora Research Institute in Inuvik, Prof Philip Marsh of Wilfrid Laurier University, Dr Oliver Sonnentag of Université de Montréal, and Dr Mark Cooper of the University of Exeter, for support during the field campaigns, Environment Canada for data access, Dr James Weedon of Vrije Universiteit Amsterdam for support with the statistical analyses, and the staff at the NERC Radiocarbon Facility (NRCF010001) and the SUERC AMS Laboratory for the ^{14}C sample processing. The authors declare no competing financial interests. Requests for additional materials and data should be sent to J F Dean.

ORCID iDs

J F Dean https://orcid.org/0000-0001-9058-7076

References

Abbott B W *et al* 2016 Biomass offsets little or none of permafrost carbon release from soils, streams, and wildfire: an expert assessment *Environ. Res. Lett.* **11** 34014

Boden T, Marland G and Andres R 2010 *Global Fossil-Fuel CO_2 Emissions* (Oak Ridge, TN: Carbon Dioxide Information Analysis Centre, Oak Ridge National Laboratory, US Department of Energy)

Bouchard F, Laurion I, Preskienis V, Fortier D, Xu X and Whiticar M J 2015 Modern to millennium-old greenhouse gases emitted from ponds and lakes of the Eastern Canadian Arctic (Bylot Island, Nunavut) *Biogeosciences* **12** 7279–98

Burn C R and Kokelj S V 2009 The environment and permafrost of the Mackenzie delta area *Permafr. Periglac. Process.* **20** 83–105

Campeau A, Bishop K, Billett M F, Garnett M H, Laudon H, Leach J A, Nilsson M B, Öquist M G and Wallin M B 2017a Aquatic export of young dissolved and gaseous carbon from a pristine boreal fen: implications for peat carbon stock stability *Glob. Change Biol.* **23** 5523–36

Campeau A, Wallin M B, Giesler R, Löfgren S, Mörth C-M, Schiff S, Venkiteswaran J J and Bishop K 2017b Multiple sources and sinks of dissolved inorganic carbon across Swedish streams, refocusing the lens of stable C isotopes *Sci. Rep.* **7** 9158

Clymo R S and Bryant C L 2008 Diffusion and mass flow of dissolved carbon dioxide, methane, and dissolved organic carbon in a 7 m deep raised peat bog *Geochim. Cosmochim. Acta* **72** 2048–66

Corbett J E, Tfaily M M, Burdige D J, Cooper W T, Glaser P H and Chanton J P 2013 Partitioning pathways of CO_2 production in peatlands with stable carbon isotopes *Biogeochemistry* **114** 327–40

Dean J F, Billett M F, Baxter R, Dinsmore K J, Lessels J S, Street L E, Subke J-A J-A, Tetzlaff D, Washbourne I and Wookey P A 2016 Biogeochemistry of 'pristine' freshwater stream and lake systems in the western Canadian Arctic *Biogeochemistry* **130** 191–213

Dean J F, Billett M F, Murray C and Garnett M H 2017 Ancient dissolved methane in inland waters revealed by a new collection method at low field concentrations for radiocarbon (^{14}C) analysis *Water Res.* **115** 236–44

Doctor D H, Kendall C, Sebestyen S D, Shanley J B, Ohte N and Boyer E W 2008 Carbon isotope fractionation of dissolved inorganic carbon (DIC) due to outgassing of carbon dioxide from a headwater stream *Hydrol. Process.* **22** 2410–23

Drake T W, Wickland K P, Spencer R G M, McKnight D M and Striegl R G 2015 Ancient low molecular-weight organic acids in permafrost fuel rapid carbon dioxide production upon thaw *Proc. Natl Acad. Sci.* **112** 13946–51

Dutta K 2016 Sun, ocean, nuclear bombs, and fossil fuels: radiocarbon variations and implications for high-resolution dating *Annu. Rev. Earth Planet. Sci.* **44** 239–75

Evans C D *et al* 2014 Contrasting vulnerability of drained tropical and high-latitude peatlands to fluvial loss of stored carbon *Glob. Biogeochem. Cycles* **28** 1215–34

Garnett M H, Billett M F, Gulliver P and Dean J F 2016a A new field approach for the collection of samples for aquatic $^{14}CO_2$ analysis using headspace equilibration and molecular sieve traps: the super headspace method *Ecohydrology* **9** 1630–8

Garnett M H, Gulliver P and Billett M F 2016b A rapid method to collect methane from peatland streams for radiocarbon analysis *Ecohydrology* **9** 113–21

Guo L, Ping C-L and Macdonald R W 2007 Mobilization pathways of organic carbon from permafrost to arctic rivers in a changing climate *Geophys. Res. Lett.* **34** L13603

Hicks Pries C E, Schuur E A G and Crummer K G 2013 Thawing permafrost increases old soil and autotrophic respiration in tundra: partitioning ecosystem respiration using $\delta^{13}C$ and $\Delta^{14}C$ *Glob. Chang. Biol.* **19** 649–61

Hicks Pries C E, Schuur E A G, Natali S M and Crummer K G 2016 Old soil carbon losses increase with ecosystem respiration in experimentally thawed tundra *Nat. Clim. Change* **6** 214–8

Holmes R M *et al* 2012 Seasonal and annual fluxes of nutrients and organic matter from large rivers to the Arctic Ocean and surrounding seas *Estuaries Coasts* **35** 369–82

Hrachowitz M and Clark M P 2017 HESS opinions: the complementary merits of competing modelling philosophies in hydrology *Hydrol. Earth Syst. Sci.* **21** 3953–73

Hua Q, Barbetti M and Rakowski A Z 2013 Atmospheric radiocarbon for the period 1950–2010 *Radiocarbon* **55** 2059–72

Jansson J K and Taş N 2014 The microbial ecology of permafrost *Nat. Rev. Microbiol.* **12** 414–25

Levin I, Kromer B and Hammer S 2013 Atmospheric $\Delta^{14}CO_2$ trend in western European background air from 2000–2012 *Tellus B Chem. Phys. Meteorol.* **65** 20092

Mann P J, Eglinton T I, McIntyre C P, Zimov N, Davydova A, Vonk J E, Holmes R M and Spencer R G M 2015 Utilization of ancient permafrost carbon in headwaters of Arctic fluvial networks *Nat. Commun.* **6** 7856

Marwick T R, Tamooh F, Teodoru C R, Borges A V, Darchambeau F and Bouillon S 2015 The age of river-transported carbon: a global perspective *Glob. Biogeochem. Cycles* **29** 122–37

McGuire A D, Anderson L G, Christensen T R, Scott D, Laodong G, Hayes D J, Martin H, Lorenson T D, Macdonald R W and Nigel R 2009 Sensitivity of the carbon cycle in the Arctic to climate change *Ecol. Monogr.* **79** 523–55

Moore S, Evans C D, Page S E, Garnett M H, Jones T G, Freeman C, Hooijer A, Wiltshire A J, Limin S H and Gauci V 2013 Deep instability of deforested tropical peatlands revealed by fluvial organic carbon fluxes *Nature* **493** 660–3

Neff J C, Finlay J C, Zimov S A, Davydov S P, Carrasco J J, Schuur E A G and Davydova A I 2006 Seasonal changes in the age and structure of dissolved organic carbon in Siberian rivers and streams *Geophys. Res. Lett.* **33** L23401

Negandhi K, Laurion I, Whiticar M J, Galand P E, Xu X and Lovejoy C 2013 Small thaw ponds: an unaccounted source of methane in the Canadian high Arctic *PLoS ONE* **8** e78204

Olefeldt D *et al* 2016 Circumpolar distribution and carbon storage of thermokarst landscapes *Nat. Commun.* **7** 13043

Paytan A, Lecher A L, Dimova N, Sparrow K J, Kodovska F G-T, Murray J, Tulaczyk S and Kessler J D 2015 Methane transport from the active layer to lakes in the Arctic using Toolik lake, Alaska, as a case study *Proc. Natl Acad. Sci.* **112** 3636–40

Quinton W L and Pomeroy J W 2006 Transformations of runoff chemistry in the Arctic tundra, northwest territories, Canada *Hydrol. Process.* **20** 2901–19

Raymond P A, McClelland J W, Holmes R M, Zhulidov A V, Mull K, Peterson B J, Striegl R G, Aiken G R and Gurtovaya T Y 2007 Flux and age of dissolved organic carbon exported to the Arctic Ocean: a carbon isotopic study of the five largest arctic rivers *Glob. Biogeochem. Cycles* **21** GB4011

Reimer P J *et al* 2013 IntCal13 and Marine13 radiocarbon age calibration curves 0–50 000 years cal BP *Radiocarbon* **55** 1869–87

Schuur E A G, McGuire A D, Grosse G, Harden J W, Hayes D J, Hugelius G, Koven C D and Kuhry P 2015 Climate change and the permafrost carbon feedback *Nature* **520** 171–9

Schuur E A G, Vogel J G, Crummer K G, Lee H, Sickman J O and Osterkamp T E 2009 The effect of permafrost thaw on old carbon release and net carbon exchange from tundra *Nature* **459** 556–9

Sierra C A, Müller M, Metzler H, Manzoni S and Trumbore S E 2017 The muddle of ages, turnover, transit, and residence times in the carbon cycle *Glob. Change Biol.* **23** 1763–73

Spencer R G M, Mann P J, Dittmar T, Eglinton T I, McIntyre C, Holmes R M, Zimov N and Stubbins A 2015 Detecting the signature of permafrost thaw in Arctic rivers *Geophys. Res. Lett.* **42** 2830–5

Street L E, Dean J F, Billett M F, Baxter R, Dinsmore K J, Lessels J S, Subke J-A J-A, Tetzlaff D and Wookey P A 2016 Redox dynamics in the active layer of an Arctic headwater catchment; examining the potential for transfer of dissolved methane from soils to stream water *J. Geophys. Res. Biogeosci.* **121** 2776–92

Vonk J E *et al* 2013a High biolability of ancient permafrost carbon upon thaw *Geophys. Res. Lett.* **40** 2689–93

Vonk J E, Mann P J, Dowdy K L, Davydova A, Davydov S P, Zimov N, Spencer R G M, Bulygina E B, Eglinton T I and Holmes R M 2013b Dissolved organic carbon loss from Yedoma permafrost amplified by ice wedge thaw *Environ. Res. Lett.* **8** 35023

Vonk J E *et al* 2015 Reviews and syntheses: effects of permafrost thaw on Arctic aquatic ecosystems *Biogeosciences* **12** 7129–67

Walker D A *et al* 2005 The circumpolar arctic vegetation map *J. Veg. Sci.* **16** 267

Walter Anthony K, Daanen R, Anthony P, Schneider von Deimling T, Ping C-L, Chanton J P and Grosse G 2016 Methane emissions proportional to permafrost carbon thawed in Arctic lakes since the 1950s *Nat. Geosci.* **9** 679–82

Ward C P and Cory R M 2015 Chemical composition of dissolved organic matter draining permafrost soils *Geochim. Cosmochim. Acta.* **167** 63–79

Wik M, Varner R K, Anthony K W, MacIntyre S and Bastviken D 2016 Climate-sensitive northern lakes and ponds are critical components of methane release *Nat. Geosci.* **9** 99–105